



HAL
open science

Insights in the Aqueous and Adsorbed Photocatalytic Degradation of Carbamazepine by a Biosourced Composite: Kinetics, Mechanisms and DFT Calculations

El Mountassir El Mouchtari, Lahoucine Bahsis, Lekbira El Mersly, Hafid Anane, Stephanie Lebarillier, Anne Piram, Samir Briche, Pascal Wong-Wah-Chung, Salah Rafqah

► To cite this version:

El Mountassir El Mouchtari, Lahoucine Bahsis, Lekbira El Mersly, Hafid Anane, Stephanie Lebarillier, et al.. Insights in the Aqueous and Adsorbed Photocatalytic Degradation of Carbamazepine by a Biosourced Composite: Kinetics, Mechanisms and DFT Calculations. *International Journal of Environmental Research*, 2021, 15 (1), pp.135-147. 10.1007/s41742-020-00300-2 . hal-03142610

HAL Id: hal-03142610

<https://hal.science/hal-03142610>

Submitted on 2 Mar 2022

HAL is a multi-disciplinary open access archive for the deposit and dissemination of scientific research documents, whether they are published or not. The documents may come from teaching and research institutions in France or abroad, or from public or private research centers.

L'archive ouverte pluridisciplinaire **HAL**, est destinée au dépôt et à la diffusion de documents scientifiques de niveau recherche, publiés ou non, émanant des établissements d'enseignement et de recherche français ou étrangers, des laboratoires publics ou privés.

Insights in the aqueous and adsorbed photocatalytic degradation of carbamazepine by a biosourced composite: kinetics, mechanisms and DFT calculations.

El Mouchtari EL mountassir^(a,c), Bahsis Lahoucine^(a,b), El Mersly Lekbira^(a), Anane Hafid^(a),
Lebarillier Stephanie^(c), Piram Anne^(c), Briche Samir^(d), Wong-Wah-Chung Pascal^(c), Rafqah Salah^{*(a)}.

^(a) Laboratoire de Chimie Analytique et Moléculaire, Faculté Polydisciplinaire de Safi, Université Cadi Ayyad, Safi Morocco

^(b) [Laboratoire de Chimie de Coordination et d'Analytique](#), Département de Chimie, Faculté des Sciences d'El Jadida, Université Chouaïb Doukkali, El Jadida, Morocco

^(c) Aix Marseille Univ, CNRS, LCE, Marseille, France

^(d) Département stockage de l'énergie et revêtements multifonctionnels, MAScIR, Rabat, Morocco.

* Corresponding author: [Pr. Salah RAFQAH](#) (E-mail : s.rafqah@uca.ma)

Laboratoire de Chimie Analytique et Moléculaire (LCAM)

Département de Chimie, Faculté Polydisciplinaire de Safi Université Cadi Ayyad.

Sidi Bouzid, B.P. 4162, 46000 Safi Maroc

Tel : 00-212-524669357 ;Fax : 00-212-524669516.

Abstract

Although the degradation of carbamazepine (CBZ) in aqueous phase was widely studied for a better comprehension of its photocatalytic behavior in the aqueous solution, the knowledge about its photodegradation adsorbed on solid surfaces is yet very limited. In this work, the combination of two processes (adsorption and photocatalysis) have been applied for degradation of CBZ adsorbed on TiO₂ and activated carbon AC/TiO₂ and aqueous phase. The degradation efficiency of CBZ could reach 100%, and 99% in CBZ dissolved and adsorbed parts, respectively. Moreover, the CBZ mineralization starts at 4 hours of irradiation. Hydroxy radical ($\bullet\text{OH}$) has an essential role in CBZ degradation, and It accompanies a synergistic effect of photogenerated [hole](#) (h^+) and [oxygen](#) active species during the reaction. Thereafter, the transformation products and possible degradation pathways of CBZ were identified by LC/MS-Qtof. Density functional theory (DFT) calculation successfully predicts the degradation mechanism of CBZ molecule by means of Fukui indexes, including the ring hydroxylation, photocyclization, C-C and C-N bond cleavage processes.

Keywords: Aqueous/adsorbed phase, Carbamazepine, Adsorption/Photocatalysis, AC/TiO₂, Mechanism, DFT.

Highlights

- **The total disappearance of CBZ in the aqueous phase and 99% degraded in the adsorbed phase.**
- **Establish the degradation kinetics of CBZ photoproducts in the dissolved and adsorbed phase.**
- **The CBZ mineralization in adsorbed and dissolved parts.**
- **The Confirmation of CBZ phototransformation mechanisms in the presence of AC/TiO₂-9% by density functional theory (DFT).**

Introduction

The past several years, pharmaceuticals have attracted considerable attention due to their residues and adverse impacts on aquatic environments (Pan et al. 2017). Wastewater treatment processes do not enable all pharmaceuticals to be efficiently eliminated, which presents risk for human health and animals even at low levels (ng.L^{-1} - $\mu\text{g.L}^{-1}$) because of their toxicity, bio-accumulation, and persistence (Chen et al. 2016; Yang et al. 2017; Bartolomeu et al. 2018). Carbamazepine (CBZ), an anticonvulsant, thyroid-regulating, and antimanic drug (Jelic et al. 2012), is one of the most frequently detected emerging contaminants in the aquatic environment, in surface water and effluent of municipal WWTPs (Qin et al. 2015; Abdel-Aziz et al. 2019). Its annual consumption is determined to be about 2,235,000 € worldwide in (Tang et al. 2017). Its removal rate in WWTPs is generally less than 10% (Zhang et al. 2008; Ali 2019). Consequently, it is necessary to study efficient and environmental-friendly technologies for eliminating these contaminants.

As one of the advanced oxidation methods (AOPs), photocatalysis has been proven to be efficient for the degradation of CBZ. Various photocatalyst have been used for CBZ removal, including TiO₂ (Doll and Frimmel 2004, 2005; Carabin et al. 2015; Fabbri et al. 2019), BiVO₄ (Tang et al. 2017), SnO₂ (Begum and Ahmaruzzaman 2018), Ag₃PO₄/AgI (Duan et al. 2019). However, difficulties with the use of powders are also well recognized: (1) aggregation of particles in suspension; (2) the loss of catalysts in the solution; (3) difficulty in application (Sopyan et al. 1996; Leary and Westwood 2011). Various supports have been adopted to immobilized TiO₂, including activated carbon (AC) (Rodríguez-reinoso 1998; Yao et al. 2010; Basha et al. 2011; Briche et al. 2020), Zeolites (Valova et al. 2010; Moosavifar and Bagheri 2019), stainless steels (Uzunova et al. 2007) and glass beads (Li Puma et al. 2008). In particular,

activated carbon has been investigated as a carrier for heterogeneous catalysts, as it is inexpensive and widely available with a relatively large surface area. It is widely used for the removal of metals (Babu and Gupta 2008; Gode et al. 2008; Chen et al. 2011; Nigam et al. 2019; Sunil et al. 2020), pesticides (Tang et al. 2020) and pharmaceuticals (Ouyang et al. 2020). Adding TiO₂ to AC was expected to induce some beneficial effects with high adsorption capacity of pollutants on AC followed by mass transfer to the photoactive TiO₂ through common interface (Matos et al. 1998, 2001; Tryba et al. 2003).

In the present study, the aim is the combination of two treatment processes: adsorption and photocatalysis to remove the pharmaceutical pollutant carbamazepine in aqueous solution. CBZ adsorbed to AC/TiO₂ was degraded by the particle of TiO₂ upon irradiation. The mechanism of degradation of carbamazepine was proposed and confirmed by density functional theory (DFT).

Materials and methods

Chemicals

Carbamazepine (99% purity) was purchased from Sigma-Aldrich (St-Louis, USA), and acetonitrile (HPLC grade) was provided by VWR chemicals (Fontenay-sous-Bois, France). Water and acetonitrile (Optima® LC/MS grade) were obtained from Fischer Scientific SAS (Fair Lawn, USA, and Geel, Belgium, respectively) and formic acid (LC/MS grade) was purchased from VWR chemical (Fontenay-sous-Bois, France). Isopropanol (IPA, 99% purity) and triethanolamine (TEOA, 98% purity) were provided by VWR chemicals and Carlo Erba (Milano, Italy).

TiO₂ and activated carbon of Argania Spinosa tree nutshells composites (TiO₂/AC) used in this study were synthesized and well characterized (chemically and physically) as previously described by El mouchtari et al. in a recent work (El Mouchtari et al. 2020). The AC-TiO₂-9% biocomposite has selected as a compromise because of its high adsorption capacity, highest degradation rate, and lowest preparation cost.

Experimental procedure and analyses

The concentration of pharmaceuticals was determined by liquid chromatography apparatus (UPLC PerkinElmer Altus 30) equipped with an Eclipse Plus C18 (3,5 μm; 2,5 × 150 mm) and

a 220/240 pump, a 330 diode array UV-visible detector, a 363 fluorescence detector and a 410 automatic injector. An isocratic method set at a flow rate of 0.25 mL/min for CBZ. The injected volume was equal to 10 μ L. The separation was obtained using a mixture of water/acetonitrile (with 0.1% formic acid) ratio of 65:35 for the analysis of CBZ. The detection of CBZ was realized using 285 nm. Before injection, samples were systematically filtered on a 0.2 μ m cellulosic filter of 15 mm in diameter and the non-retention of pharmaceutical compounds on filters has been tested. The filter purchased by Agilent Technologies was used to remove the photocatalyst.

Identification of carbamazepine degradation products was performed by liquid chromatography coupled with high-resolution tandem mass spectrometry (LC-MS QTOF), using Agilent 1290 Infinity a reversed-phase column (Zorbax Eclipse Plus C18, 1.8 μ m; 2.1 \times 50 mm) distributed by Agilent was used at a flow rate of 0.4 mL.min⁻¹. The elution gradient was modified to elute all transformation products while the column and flow rate remained unchanged. 20 μ L samples are injected into the LC system using ACN/H₂O (5/95) acidified with 0.1%v formic acid (solvent A) and ACN/H₂O (95/5) acidified with 0.1% formic acid (solvent B) with the following gradient: 0-0.4 min 5.3% A, 0.4-3 min 10.5%, 3-7 min 35.8% B. The source parameters were established as follows: fragmenter: 140 V, capillary voltage: 3000 V, skimmer 65 V, nebulizer pressure (30 psi), nebulizer needle voltage (500 V), nitrogen was used as desolvation gas (temperature 350°C, flow rate 10 L.min⁻¹), and the flow rates for the sheath gas were set at 350°C and 8 L.min⁻¹ respectively. The solutions studied were injected as is or after reconcentration by a factor of 5 or 10 by evaporation under air flow at 40°C and analysed in simple mass spectrometry mode (ToF, mass resolution on the ion of m/z = 922 of 9382 \pm 317) and in MS/MS mode (QqToF) in some cases depending on the abundance of the fragments. In the first case, ion acquisition was performed for m/z ratios ranging from 100 to 1000 amu with 10,000 transients per spectrum. The analytes were ionized in positive mode. In the second case, the precursor ions were subjected to three collision energies (10, 20 and 40 eV), and the acquisition of the daughter ions was performed at m/z ratios ranging from 50 to 1000 amu.

Protocol extraction of the adsorbed phase

For each adsorption experience, 0.1 g.L⁻¹ of AC-TiO₂-9% was dispersed in 50 mL CBZ aqueous solution (50 mg.L⁻¹) in dark condition at 25 °C. A magnetic stirring was maintained at 400 rpm for 2h until the adsorption/desorption equilibrium was attained. After equilibration, the mixture was centrifuged at 4000 rpm for 2 min, and then the supernatant was recovered. LC analysis

allowed to determine the concentration of CBZ in the supernatant and the quantity of CBZ adsorbed was calculated from the difference between the beginning and equilibrium concentration of CBZ. After irradiation, every sample was centrifuged and the supernatant analyzed by LC to evaluate the concentration of degraded CBZ in the aqueous phase. Then, the solid residues were recovered, dried under the hood for 24 hours, next the solid residues were extracted with 50 mL of methanol solution. The presence of methanol in the extraction solution could efficiently desorb the CBZ adsorbed in the AC-TiO₂-9%. The extraction solution containing the solid residue was magnetically stirring for 2 hours min. After filtration, the methanol was evaporated in a Turbovap evaporator at 40°C with nitrogen gas. The recovered CBZ was then dissolved in 50 mL of ultra-pure water. All steps of this extraction protocol were repeated three times to ensure the extraction of all CBZ and its products were extracted. The LC analysis showed that such extraction ensured around 95% (94.69±0.74%) recovery of CBZ (table S1). The recovery of CBZ was calculated from the ratio of the amount of CBZ in extraction solution to that adsorbed on AC-TiO₂-9%.

Computational details

To predict the mechanism of degradation and byproducts of carbamazepine, density functional theory (DFT) calculations were performed with the Gaussian 09W program package. The B3LYP functional with a 6-31G(d,p) basis set was applied to optimize the geometries of carbamazepine and all intermediates / products. Frequency calculations were performed to verify the stationary points to be real minima. The solvent effect was described by the CPCM solvent model using water as a solvent (Tomasi and Persico 1994). Moreover, the Fukui function was used to predict the electrophilic and nucleophilic sites (see Supplementary material for more details) (Ayers and Parr 2000).

Result and discussion

Photocatalytic study

The photocatalytic performance of AC-TiO₂-9% was obtained by monitoring the degradation of CBZ adsorbed on AC-TiO₂-9% and in the aqueous phase. The results are shown in Figure 1.

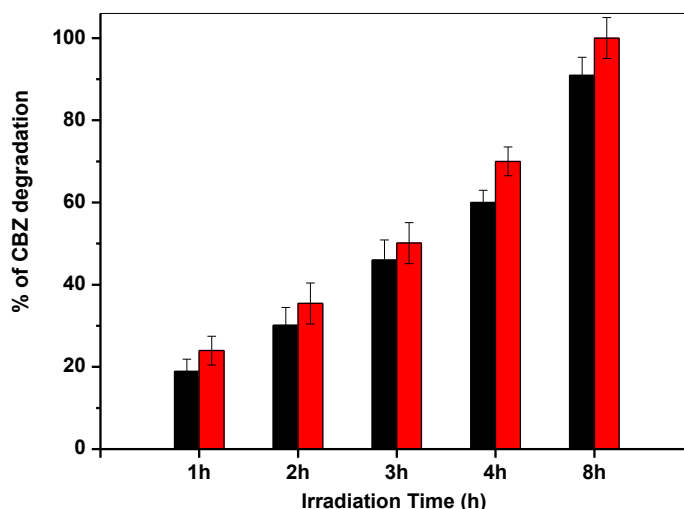


Fig 1. CBZ degradation kinetics in adsorbed (black) and aqueous (red) phase by AC-TiO₂-9% [CBZ] = 50 mg.L⁻¹, [AC-TiO₂-9%] = 0.1 g.L⁻¹, Xe lamp 300W

Whatever the irradiation time, one can notice that the elimination of CBZ is always greater in the aqueous phase than that in the adsorbed one. For instance, it can be observed, on the one hand, that after 8 hours upon irradiation, the total disappearance of CBZ in solution, on the other hand, there is very little amount of CBZ in the adsorbed phase on AC/TiO₂-9% after 8 hours.

These results could be explained by different process. First, as CBZ disappearance occurs at the surface of the photocatalyst, the concentration of CBZ at the surface of AC/TiO₂-9% decreases more slowly than the one in solution because the adsorption sites made available during CBZ degradation are immediately occupied by new molecules of CBZ coming from the aqueous phase. Moreover, the adsorption competition between carbamazepine and its photoproducts formed in the solution on the surface of AC/TiO₂-9% and their concomitant degradation could also be responsible of such difference. In fact, as shown in Figure 2, more compounds in higher concentration have been detected in the adsorbed phase, suggesting that byproducts are mainly adsorbed.

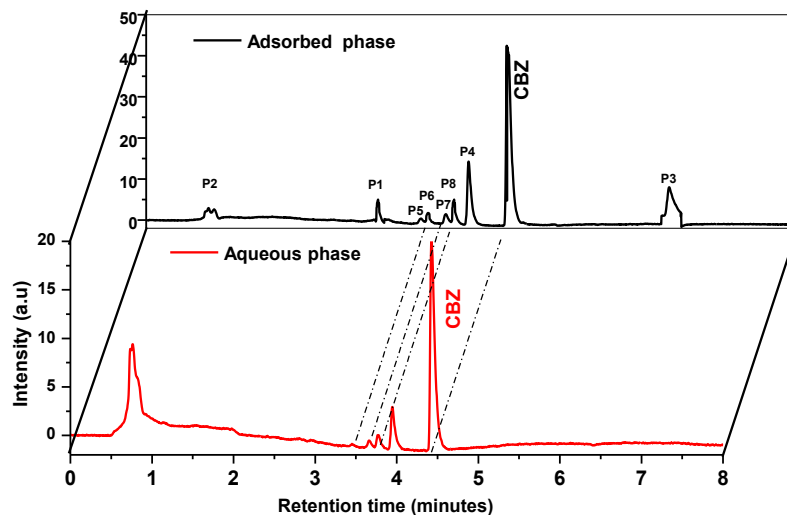
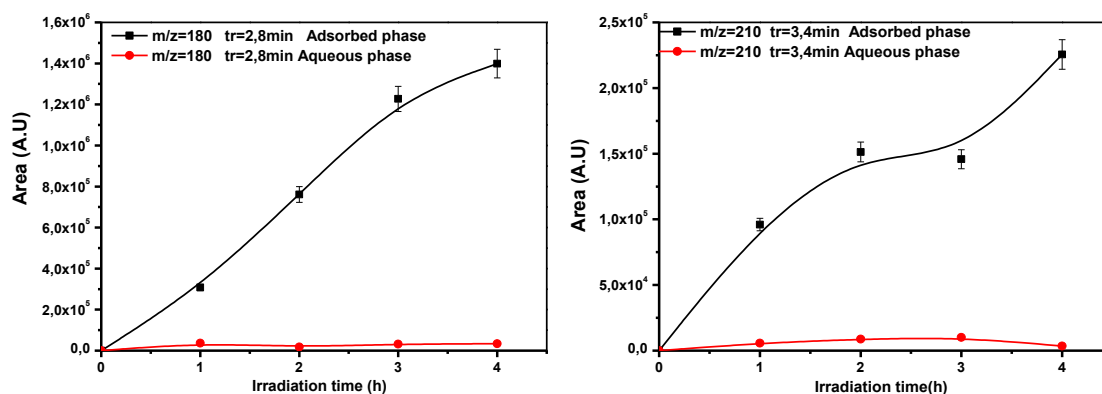


Fig 2. HPLC Chromatogram of the adsorbed and aqueous phase of solution of CBZ and AC-TiO₂-9% after 4h upon irradiation. [CBZ] = 50 mg.L⁻¹, [AC-TiO₂-9%] = 0.1 g.L⁻¹, Xe lamp 300W, λ_{detection} = 285 nm.

The formation kinetics of some byproducts detected in both phases are plotted as a function of the irradiation in figure 3. It is clearly observed that these products have a high affinity for the surface of AC-TiO₂ since their concentration appeared higher after extraction compared to that detected in the aqueous phase, which is relatively low. Moreover, we can notice that the absence of some byproducts (P7 and P8) in the aqueous phase is explained by their migration to the adsorbed phase, thus suggesting their **removal** from the aqueous medium.



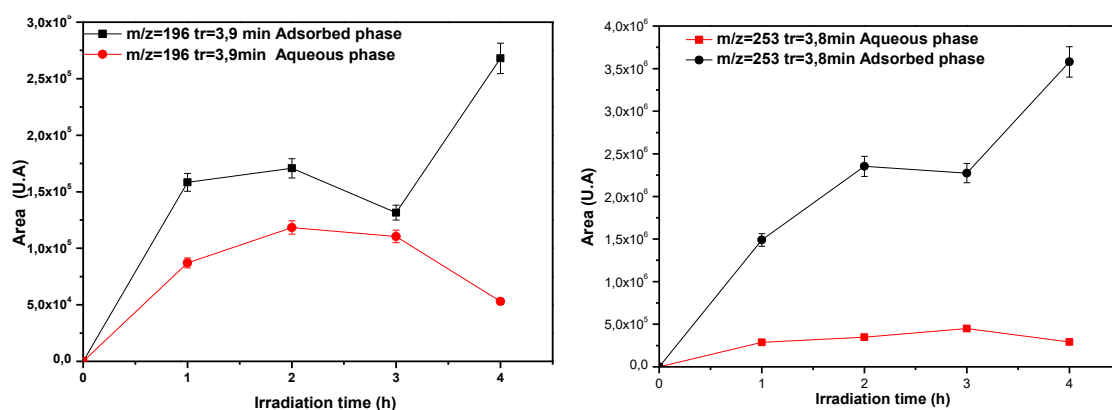


Fig 3. Kinetics of degradation of the TPs detected in aqueous solution (red) and adsorbed on AC-TiO₂-9% (black).

Identification of transformation product

To identify CBZ transformation products (TPs) in the presence of AC-TiO₂-9%, we focused our analyses on samples taken after irradiation times of 60, 120, 180 and 240 minutes with a CBZ degradation rate of about 70% after 240 min irradiation in aqueous phase. This identification was performed using LC-MS-QToF in positive mode. We first determined for each TP the exact mass to propose a raw formula taking into account isotopic distribution and the lowest mass difference between the proposed formula and the actual measured mass. In a second approach, MS-MS experiments were realized and the accurate mass of each fragment was measured and raw formula was identically proposed. The list of identified photoproducts in the two phases (adsorbed and aqueous) is presented in **Table 1**.

The product P1 at m/z 180.0806 is fragmentation leads to the obtention of two fragment ions. The first fragment ion of m/z equal to 152 corresponds to a loss of a C₂H₄ group (28 Da), and the second of m/z corresponding to 128 (52 Da) corresponds to a loss of the C₄H₄. This product was allocated in the literature to acridine (Jelic et al. 2012). The product P2 at m/z 224, with a molecular formula C₁₄H₉NO₂, shows the loss of the amine function (NH₂) and a carbon atom that can be explained by a ring hydroxylation followed by a ring contraction. It corresponds to the acridone-N-carbaldehyde shown in Table 1, as suggested by S. Begum et al.. (Begum and Ahmaruzzaman 2018).

Product P4 was identified with m/z 196.0762 suggested an elemental composition of C₁₃H₉NO, which conduct to the formation of a single m/z fragment equal to 167 by MS-MS analysis. This fragment corresponds to a loss of a CHO group in the acridone molecule as already identified (Jelic et al. 2012).

Product P5 with m/z 271.1078 generated by a double hydroxylation process. Its fragmentation conduct to the production of 4 ions with a m/z ratio equal to 253, 236, 210 and 180 as shown in the table below. This fragmentation mechanism highlights the following processes: the loss of a water molecule, the amine function, the amide function and finally CH_2O which leads to the contraction of the 7-cycle (azepine) as described in the literature (Miao and Metcalfe 2003). Thus, P5 could be attributed to 10, 11-Dihydroxy-carbamazepine.

For P8, three compounds (P8-a, P8-b, and P8-c) were identified with the same m/z equal to 253.098, assigned to $\text{C}_{15}\text{H}_{12}\text{N}_2\text{O}_2$ elementary composition. Several structural proposals have been suggested in the literature giving identical fragment ions, that did not allow an unambiguous structure attribution (Miao and Metcalfe 2003; Kosjek et al. 2009; Hübner et al. 2014). However, MS/MS experiments on P8-a and P8-c photoproducts show the production of three fragment ions with $m/z = 236, 210, \text{ and } 180$. These fragmentations are due to losses of NH_3 , HCNO and CO_2 followed by a loss of H_2CO , respectively. This product corresponds to hydroxycarbamazepine (CBZ-OH). Two works report that the presence of these fragments can also be attributed to 10,11-dihydro-10,11 epoxycarbamazepine (EPOCBZ) and acridine 9 carboxyaldehyde (Miao and Metcalfe 2003; Calza et al. 2012). For CBZ-OH, there are two possible P8-a1 and P8-a2 isomers, so a DFT study was undertaken to determine the exact position of the OH^* attack (table 2).

P7 with m/z 251.082 was assigned to CBZ ketone derivative based on the results obtained by Jelic and Michael (Jelic et al. 2013). In fact, the fragmentation of this product generates the fragment ion of m/z 223 which corresponds to the loss of 28 Da confirming the presence of a carbonyl group.

To elucidate the structure of P3 with m/z 226.0706, MS^2 results were considered with the detection of two fragment ions under our operating conditions. The first with a m/z ratio equal to 208 corresponds to the loss of one molecule of water (18 Da) from the precursor molecular ion. The other fragment ion with a m/z ratio of 180, which corresponds to a loss of HCO (28 Da), shows the existence of a carbonyl function on the acridine. Which enables the validation of the structural proposal of a derivative P3 is hydroxyl-(9H,10H)-acridine-9-carboxyaldehyde(9-CA-ADIN).

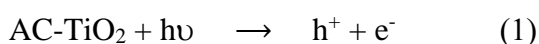
Table1. Transformation products of CBZ identified in samples, retention time (R_t), accurate mass in EC^+/MS ($[\text{M}+\text{H}]^+$), masse difference (ΔM), molecular formula, fragment accurate masse in EC^+/MS^2 ($[\text{M}+\text{H}]^+ \text{MS}^2$), assigned formula and proposal structure.

Product	R _t , min	[M+H] ⁺ m/z	ΔM	Molecular Formula	[M+H] ⁺ MS ²	Assigned Formula	Structure proposal
CBZ	4,4	237.1025	-	C ₁₅ H ₁₂ N ₂ O	-	-	
P1	2,8	180.0807	-57,0208	C ₁₃ H ₉ N	152.0976 128.0507	C ₁₁ H ₆ N ⁺ C ₉ H ₆ N ⁺	
P2	0,75	224.0706	-13,0319	C ₁₄ H ₉ NO ₂	-	-	
P3	6,4	226.0861	-11,0164	C ₁₄ H ₁₂ NO ₂	208.0748 180 0795	C ₁₄ H ₁₀ NO C ₁₃ H ₁₀ N	
P4	3,9	196.075 6	-41.0269	C ₁₃ H ₉ NO	167.0705	C ₁₂ H ₉ N	
P5	3,38	271.1077	+34.0052	C ₁₅ H ₁₄ N ₂ O ₃	253.0966 236.0699 210.0907 180.0797	C ₁₅ H ₁₃ N ₂ O ₂ C ₁₅ H ₁₀ NO ₂ C ₁₄ H ₁₂ NO C ₁₃ H ₁₀ N	
P6	3,46	210.093 8	-43,0042	C ₁₄ H ₁₁ NO	-	-	
P7	3,66	251.082	+13.9795	C ₁₅ H ₁₁ N ₂ O ₂	-	-	
P8-a1 P8-a1' P8-a2 P8-b P8-C	3,8 3,7 3,7	253.098	+15.9951	C ₁₅ H ₁₂ N ₂ O ₂	236.0707 210.0914 180.0805	C ₁₅ H ₉ NO ₂ C ₁₄ H ₁₁ NO C ₁₃ H ₉ N	

Elucidation of reaction species implied in degradation with AC-TiO₂-9%

The synergistically improved photocatalytic activity may be explained by the adsorption of CBZ on AC-TiO₂-9%. AC has no photocatalytic activity, but it has a high adsorption capacity, which allows the transfer of CBZ from the aqueous phase to around TiO₂, which increases their photocatalytic activity. Adsorption of reactive substances on the catalyst surface is an essential step in the photocatalytic process (Maira et al. 2001; Grzechulska and Morawski 2002). AC in contact with TiO₂ is capable of prolonging the separation lifetime of photogenerated e⁻/h⁺, thus increasing the rate of OH[•] radical generation by photocatalyst. Activated carbon can act as a center where organic pollutants were adsorbed before being transferred to the degradation center (Wei et al. 2014).

To elucidate the nature of the reactive species photogenerated and responsible for degradation of CBZ in AC-TiO₂-9%, two chemical traps were employed as scavengers of hydroxyl radicals (OH[•]) and positive holes (h⁺), namely, isopropanol (IPA) and triethanolamine (TEOA) respectively (Asmus et al. 1973; Yoon and Lee 2005; Yan et al. 2010). To demonstrate the involvement of these radicals, a mixture of CBZ and AC-TiO₂-9% (50 mg.L⁻¹ and 0.1g.L⁻¹) with 2% v/v IPA or 2% v/v TEOA were irradiated under the same conditions. To determine the effect of oxygen on the degradation of CBZ, oxygen bubbling was realized before and during the irradiation experiment..As it can be observed in fig.4, the addition of IPA as well as TEOA inhibits the degradation of carbamazepine. The above results suggest that OH[•] were the principal reactive active species in the photocatalytic reaction process, and are generated by the positive holes according to the reaction (2) (Zhu et al. 2018; Al-Mamun et al. 2019). On the contrary, there's a total disappearance of the CBZ with oxygen bubbling after 4 hours of irradiation. This implies that O₂ an essential role in the degradation of carbamazepine. It enables the generation of superoxide radical O₂^{-•} by reaction 3, which can subsequently produce rise to hydroxyl radicals that are responsible for the degradation of CBZ (reaction 4). It also participates in slowing down the electron-hole recombination phenomenon, which increases photocatalytic activity (Gerischer and Heller 1991; Friedmann et al. 2010).



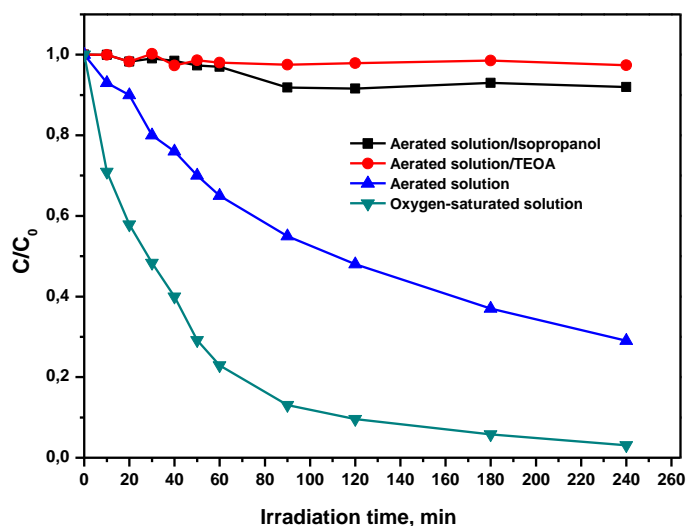
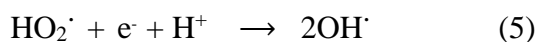
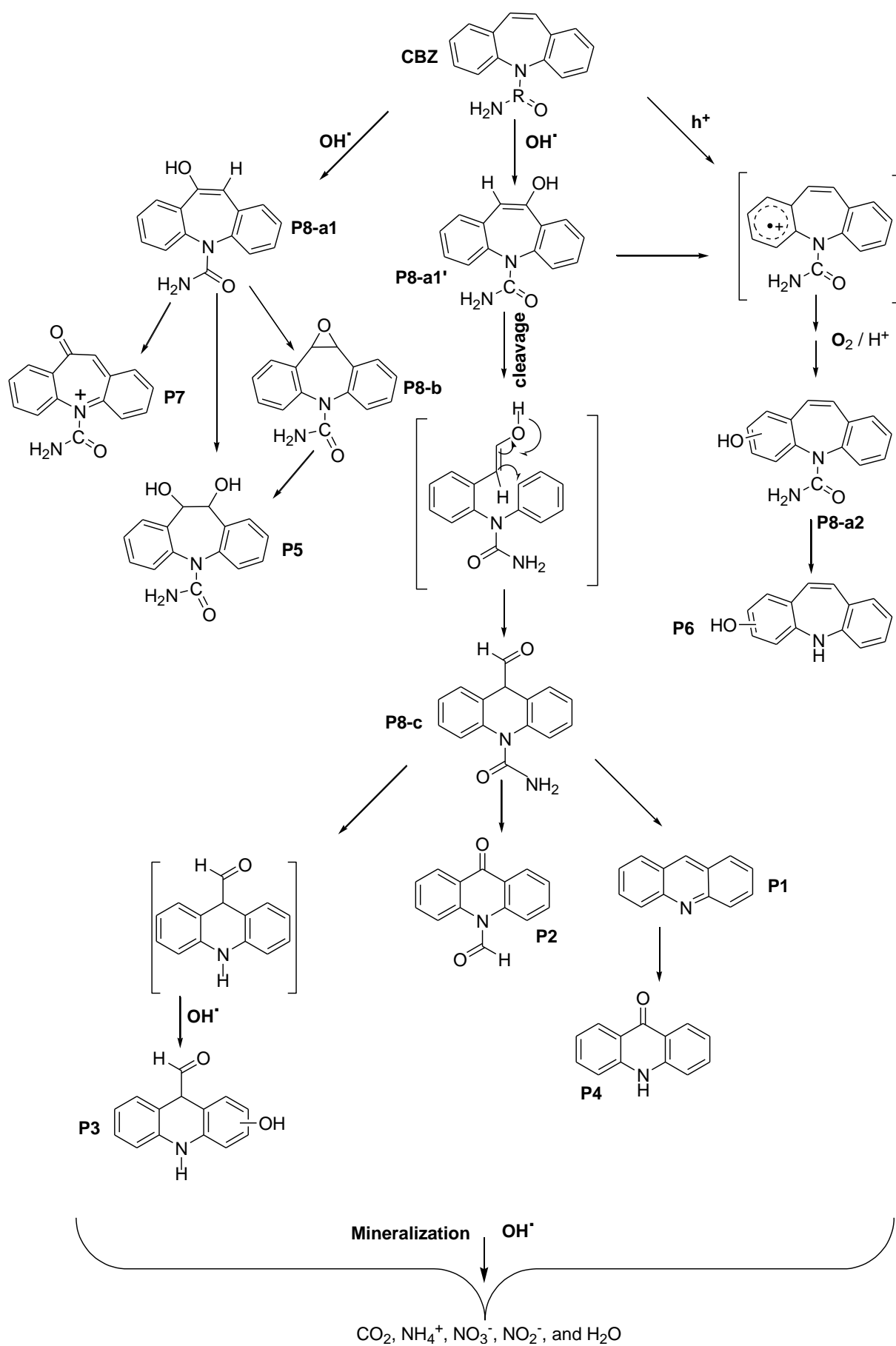


Fig 4. CBZ degradation kinetic in aerated (blue) and oxygen saturated (green) conditions and in the presence of isopropanol (black) and TEOA (red), $[\text{CBZ}] = 50 \text{ mg.L}^{-1}$, $[\text{AC-TiO}_2\text{-9\%}] = 0.1 \text{ g.L}^{-1}$, Xe lamp 300W,

We previously demonstrated the generation of hydroxyl radicals and photogenerated of positive holes involved in the degradation of carbamazepine by AC-TiO₂-9% composite material under [simulated](#) solar irradiation. This suggests that the primary step is the formation of the cation radical CBZ^{•+} by electron transfer from carbamazepine to the (h⁺) holes as proposed in scheme 1. Firstly, the formed •OH directly attacked carbon atom of the aromatic ring of CBZ^{•+} to produce P8-a1, P8-a1' and P8-a2 (monohydroxy), which are isomers differing by the position of the •OH attack in the aromatic ring as will be determined by the DFT method (Table2) (Xu et al. 2013). Meanwhile, the hydroxyl radical reacted with the olefinic double bond on the central seven-membered ring of CBZ generated the product P8-b (Ahmed and Chiron 2014). After that, product P8-b underwent a hydrolysis step to produce P5 (Ahmed and Chiron 2014). Product P7 formed by oxidation of the alcohol function of P8-a1 (Jelic et al. 2013). The product P6, generated by the loss of -CONH₂ from the product P8-a2. P8-c probably originated from P8-a1' through a ring contraction driving to N-aminocarbonylacridine-carboxaldehyde according to mechanism proposed by Chiron et al (Chiron et al. 2006). The product P8-c can be further produced by three different ways. One way is the loss of the amide

side chain followed by hydroxylation at the aromatic ring to form P3 (Petrovic et al. 2007). The other two ways are of the formation of P1 after the disappearance of both the amide team chain and the carbonyl group, this product, in turn, undergoes attack by hydroxyl radicals and then oxidation to obtain the product P4. The detection of P2 can be explained by a loss of both amine and carbonyl functions, followed by an attack by hydroxyl radicals. We conclude that all the intermediates would be mineralized to CO_2 , NH_4^+ $\text{NO}_3^-/\text{NO}_2^-$ and H_2O with enough AC/TiO₂-9% (Nawaz et al. 2017) .



Scheme 1. CBZ phototransformation mechanisms in the presence of AC/TiO₂-9%

Proposed degradation pathways of CBZ by AC-TiO₂-9%

To gain more insights into the degradation pathways of carbamazepine by AC-TiO₂ under light irradiation, LC-MS analysis and density functional theory (DFT) calculations were investigated. The degradation pathways were elucidated by the analysis of the Fukui index representing the most electrophilic (f_k^-) and radical attack (f^0) sites of the atoms on CBZ molecule. From the analysis of the detected intermediates and DFT calculations, a degradation pathway of CBZ by AC-TiO₂-9% is proposed in **Scheme 1** and the results of calculated Fukui functions were summarized in **Table 2**. The Fukui function dual descriptors are shown in Fig. 5 indicating electron acceptor sites (in purple) and electron donor sites (in blue).

The initial steps of the degradation are located in the hydroxylation of the heterocycle ring and C-C cleavage. For the ring hydroxylation, the atom C2 of CBZ molecule has a hold relative larger f_k^- (0.0938) and f^0 (0.0902) values which is more vulnerable site for OH radical attack (**Table 2**), leading to the formation of hydroxylated CBZ (P8-a1 with $m/z = 253.098$) (**Fig. 5**). Further, P8-a1 was converted into P8-b intermediate by epoxidation of the hydroxyl group (Liu et al. 2016). The analysis of Fukui function on P8-a1 shows a favorable interaction between the oxygen atom (O31) which is an important electrophilic site ($f_k^- = 0.09729$) and the carbon atom (C1) is more nucleophilic site ($f_k^+ = 0.12677$), explaining the formation of P8-b intermediate (see **Table 2; Fig. 5**). Also, the P8-a1 intermediate shows that the C1 has a larger f^0 (0.10301) value which is a favorable site for OH radical attack leading to the formation of P5 intermediate or by the hydrolysis of P8-b intermediate (Xu et al. 2013; Zhao et al. 2020). For the hydroxylation of ring phenyl, the C22 atom of CBZ molecule has a high f_k^- (0.0911) and f^0 (0.0879) values that are subsequently easy to be attacked by OH radical, conducting to the formation of P8-a2 (**Fig. 5**). Then intermediate P8-a2 undergoes amide loss forming P6 compound (Arulsamy and Bohle 2000). For the cleavage of C-C bond, the rearrangement of the intermediate P8-a1' leads to the formation of P8-c with a six-member ring. The free energy of the formation of the P8-c intermediate is exothermic by ca. 12.58 kcal.mol⁻¹, which confirms that P8-c is more stable than P8-a1' intermediate. The deamidation process of P8-c conducted to P2, P3 and P1 intermediates, therefore, these products were also observed in the biodegradation of carbamazepine (Golan-Rozen et al. 2015) excepted the P3 product. Besides, the atom C6 is the favorable site to radical attacks with a f^0 (0.09053) indicating the formation of P3 (see **Fig. 5** and **Table S2** in Supplementary material). The carbon atom C7 of the intermediate P1 has a larger f^0 (0.1178) that attached hydroxyl radicals and then oxidation to obtain the product P4 to obtain the product P4 (see **Fig.5**, **Table S3** in Supplementary material) (Zhai et al. 2018).

Finally, all mentioned intermediates will be attacked by hydroxyl radicals and then mineralized into CO₂ and H₂O molecules.

Table 2. Fukui index distribution on CBZ and P8-a1 intermediate calculated at B3LYP/6-31G(d,p) level.

Num.	Atom	CBZ			P8-a1		
		f_k^+	f_k^-	f_0	f_k^+	f_k^-	f_0
1	C	0.1161	0.0633	0.0897	0.12677	0.07925	0.10301
2	C	0.0867	0.0938	0.0902	0.0484	0.10192	0.07516
3	C	0.0309	0.0097	0.0203	0.04587	-0.00624	0.019815
4	C	0.0023	0.0366	0.0195	-0.00083	0.02658	0.012875
5	C	0.0500	0.0238	0.0369	0.05787	0.01144	0.034655
6	C	0.0387	0.0291	0.0339	0.02898	0.04267	0.035825
9	N	-0.0169	0.0692	0.0261	-0.01703	0.03469	0.00883
10	C	0.0078	0.0017	0.0048	0.0069	0.00893	0.007915
12	C	0.1002	0.0756	0.0879	0.11291	0.05963	0.08627
14	C	0.0362	0.0318	0.0340	0.04746	0.026	0.03673
16	C	0.0247	0.0259	0.0253	0.02406	0.02179	0.022925
18	C	0.0383	0.0314	0.0349	0.03764	0.03871	0.038175
20	C	0.0187	0.0294	0.0241	0.01772	0.02119	0.019455
22	C	0.0847	0.0911	0.0879	0.07931	0.09965	0.08948
24	C	0.0077	-0.0003	0.0037	0.01012	0.0007	0.00541
26	C	-0.0005	-0.0120	-0.0063	-0.00061	-0.00897	-0.00479
27	O	0.0322	0.0603	0.0463	0.0347	0.04359	0.039145
28	N	0.0075	0.0243	0.0159	0.00683	0.01937	0.0131
31	O	-	-	-	0.00205	0.09729	0.04967

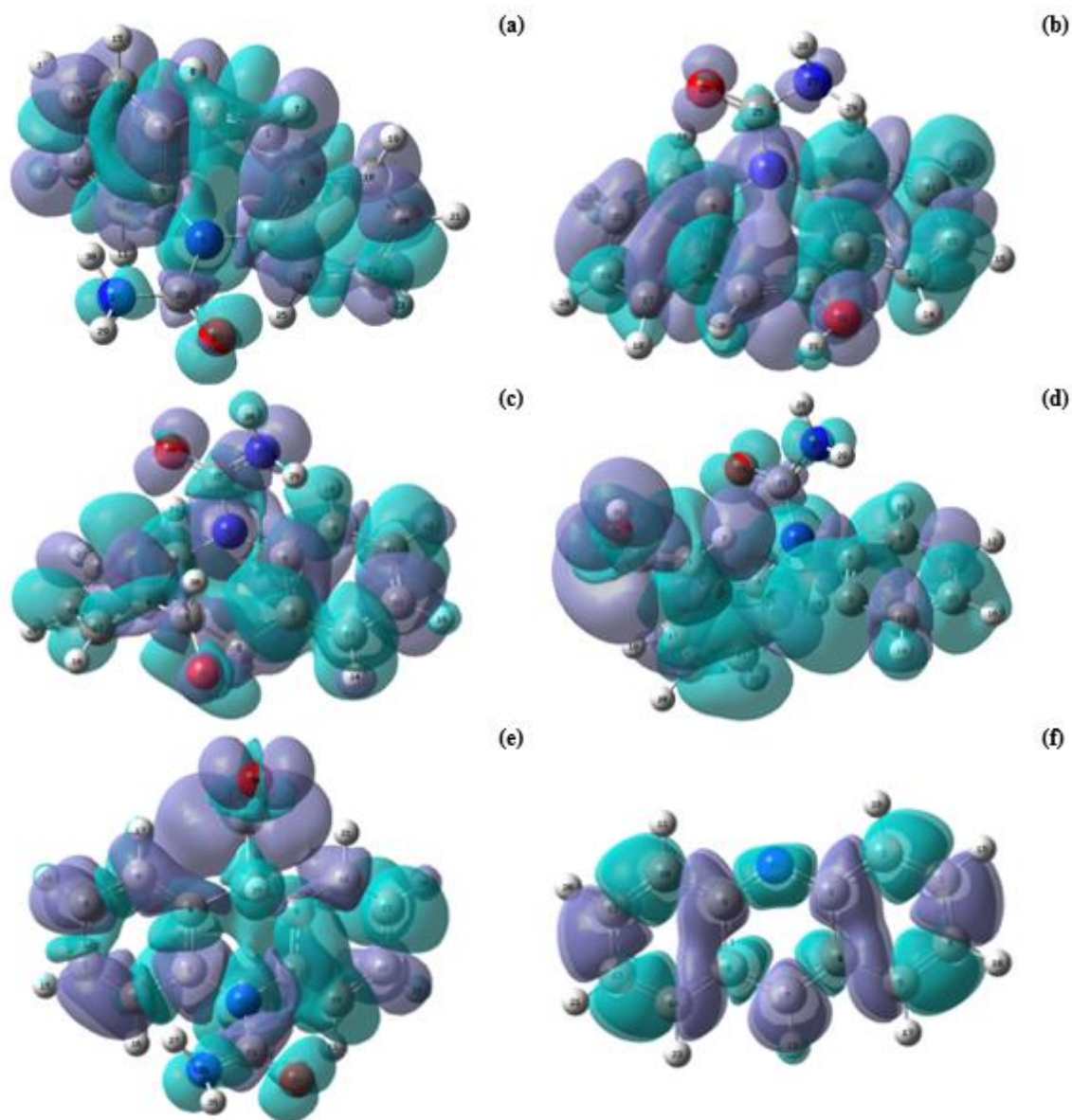


Fig 5. The dual descriptor Fukui functions for CBZ (a), P8-a1 (b), P8-b (c), Int. (d), P8-c (e) and P1 (f), respectively. For more details see the Supplementary material.

Mineralization

The kinetics of the total mineralization of CBZ was followed in both phases using the total organic carbon (TOC) analysis (Fig 6). In the presence of AC/TiO₂-9% and before irradiation, the preliminary step of adsorption leads to the removal of 50% of CBZ from the solution. That is to say, 25 ppm has transferred to the surface of ACP/TiO₂-9% and the same amount remained in the solution, both concentration were taken as reference. As presented in figure 6, the mineralization of CBZ is observed after 4 hours under irradiation at the surface of AC/TiO₂-9% but also in the solution even if CBZ is not totally degraded (70% degradation).

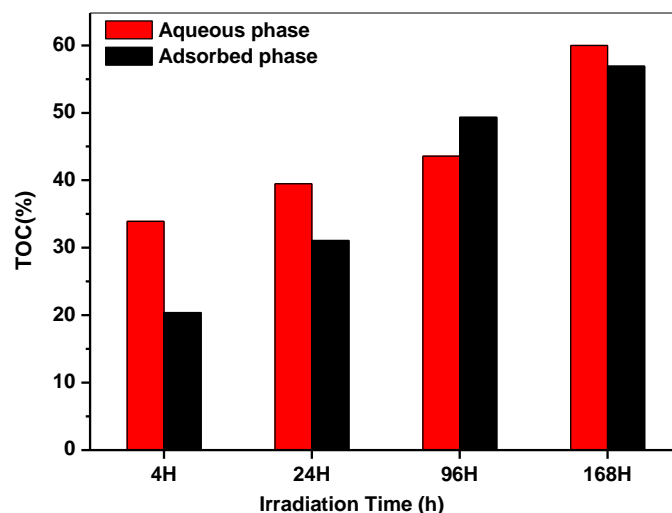


Fig 6. The evolution of TOC as a function of irradiation time in aqueous (red) and adsorbed (black) phase, [CBZ] = 50 mg.L⁻¹ ; [AC/TiO₂-9%] = 0.1 g.L⁻¹, Xe 300 W, aerated conditions.

Conclusion

AC/TiO₂-9% composite reported to be an efficient photocatalyst for elimination of carbamazepine. CBZ disappearance occurs in the aqueous and adsorbed phase with a favoured elimination in the solution and an efficient adsorption and degradation of CBZ photoproducts by a mass transfer to photoactive TiO₂. Thus, AC/TiO₂-9% composite allows the total decontamination of the aqueous phase but also its regeneration upon irradiation making it a very promising material for WWTPs. CBZ photocatalytic degradation occurs through the main participation of h⁺ and generated •OH and CBZ degradation pathway was deeply investigated through the identification of degradation intermediates and Fukui indexes in both phase.

Conflicts of interest

There are no conflicts to declare.

Acknowledgement

The authors gratefully acknowledge, Center for Analysis and Characterization of Université Cadi Ayyad, CNRST and the support by the Service de Coopération et d'Action Culturelle of the French Embassy and for funding this research through a PhD grant, for the CEDocs 2018 project.

Supporting materials

Table S1. Recovery of CBZ by extraction with MeOH

Fig S1. Kinetics of degradation of the TPs detected in aqueous solution and adsorbed on AC-TiO₂-9%.

Table S2. Fukui index distribution on P8-C calculated at B3LYP/6-31G(d,p) level.

Table S3. Fukui index distribution on P1 intermediate calculated at B3LYP/6-31G(d,p) level.

(Babu and Gupta 2008; Gode et al. 2008; Chen et al. 2011; Nigam et al. 2019; Sunil et al. 2020), pesticides (Tang et al. 2020) and pharmaceuticals(Ouyang et al. 2020)

References

- Abdel-Aziz HM, Farag RS, Abdel-Gawad SA (2019) Carbamazepine Removal from Aqueous Solution by Green Synthesis Zero-Valent Iron/Cu Nanoparticles with Ficus Benjamina Leaves' Extract. *International Journal of Environmental Research* 13:843–852. <https://doi.org/10.1007/s41742-019-00220-w>
- Ahmed MM, Chiron S (2014) Solar photo-Fenton like using persulphate for carbamazepine removal from domestic wastewater. *Water Research* 48:229–236. <https://doi.org/10.1016/j.watres.2013.09.033>
- Ali AH (2019) Removal of Sulfamethoxazole, Sulfapyridine and Carbamazepine, from Simulated Wastewater Using Conventional and Nonconventional Adsorbents. *International Journal of Environmental Research* 13:487–497. <https://doi.org/10.1007/s41742-019-00192-x>
- Al-Mamun MR, Kader S, Islam MS, Khan MZH (2019) Photocatalytic activity improvement and application of UV-TiO₂ photocatalysis in textile wastewater treatment: A review. *Journal of Environmental Chemical Engineering* 7:103248. <https://doi.org/10.1016/j.jece.2019.103248>
- Arulsamy N, Bohle DS (2000) Nucleophilic Addition of Hydroxylamine, Methoxylamine, and Hydrazine to Malononitrileoxime. *The Journal of Organic Chemistry* 65:1139–1143. <https://doi.org/10.1021/jo991614t>
- Asmus KD, Moeckel H, Henglein A (1973) Pulse radiolytic study of the site of hydroxyl radical attack on aliphatic alcohols in aqueous solution. *The Journal of Physical Chemistry* 77:1218–1221. <https://doi.org/10.1021/j100629a007>
- Ayers PW, Parr RG (2000) Variational Principles for Describing Chemical Reactions: The Fukui Function and Chemical Hardness Revisited. *Journal of the American Chemical Society* 122:2010–2018. <https://doi.org/10.1021/ja9924039>
- Babu BV, Gupta S (2008) Adsorption of Cr(VI) using activated neem leaves: kinetic studies. *Adsorption* 14:85–92. <https://doi.org/10.1007/s10450-007-9057-x>
- Bartolomeu M, Neves MGPM, Faustino MAF, Almeida A (2018) Wastewater chemical contaminants: remediation by advanced oxidation processes. *Photochemical & Photobiological Sciences* 17:1573–1598. <https://doi.org/10.1039/C8PP00249E>
- Basha S, Barr C, Keane D, et al (2011) On the adsorption/photodegradation of amoxicillin in aqueous solutions by an integrated photocatalytic adsorbent (IPCA): experimental studies and kinetics analysis. *Photochemical & Photobiological Sciences* 10:1014. <https://doi.org/10.1039/c0pp00368a>
- Begum S, Ahmaruzzaman M (2018) CTAB and SDS assisted facile fabrication of SnO₂ nanoparticles for effective degradation of carbamazepine from aqueous phase: A systematic and comparative study of their degradation performance. *Water Research* 129:470–485. <https://doi.org/10.1016/j.watres.2017.11.031>
- Briche S, Derqaoui M, Belaiche M, et al (2020) Nanocomposite material from TiO₂ and activated carbon for the removal of pharmaceutical product sulfamethazine by combined adsorption/photocatalysis in aqueous media. *Environmental Science and Pollution Research* 27:25523–25534. <https://doi.org/10.1007/s11356-020-08939-2>

- Calza P, Medana C, Padovano E, et al (2012) Identification of the unknown transformation products derived from clarithromycin and carbamazepine using liquid chromatography/high-resolution mass spectrometry: LC/HRMS for characterization of unknown compounds. *Rapid Communications in Mass Spectrometry* 26:1687–1704. <https://doi.org/10.1002/rcm.6279>
- Carabin A, Drogui P, Robert D (2015) Photo-degradation of carbamazepine using TiO₂ suspended photocatalysts. *Journal of the Taiwan Institute of Chemical Engineers* 54:109–117. <https://doi.org/10.1016/j.jtice.2015.03.006>
- Chen J, Qu R, Pan X, Wang Z (2016) Oxidative degradation of triclosan by potassium permanganate: Kinetics, degradation products, reaction mechanism, and toxicity evaluation. *Water Research* 103:215–223. <https://doi.org/10.1016/j.watres.2016.07.041>
- Chen S, Yue Q, Gao B, et al (2011) Removal of Cr(VI) from aqueous solution using modified corn stalks: Characteristic, equilibrium, kinetic and thermodynamic study. *Chemical Engineering Journal* 168:909–917. <https://doi.org/10.1016/j.cej.2011.01.063>
- Chiron S, Minero C, Vione D (2006) Photodegradation Processes of the Antiepileptic Drug Carbamazepine, Relevant To Estuarine Waters. *Environmental Science & Technology* 40:5977–5983. <https://doi.org/10.1021/es060502y>
- Doll TE, Frimmel FH (2005) Photocatalytic degradation of carbamazepine, clofibric acid and iomeprol with P25 and Hombikat UV100 in the presence of natural organic matter (NOM) and other organic water constituents. *Water Research* 39:403–411. <https://doi.org/10.1016/j.watres.2004.09.016>
- Doll TE, Frimmel FH (2004) Kinetic study of photocatalytic degradation of carbamazepine, clofibric acid, iomeprol and iopromide assisted by different TiO₂ materials—determination of intermediates and reaction pathways. *Water Research* 38:955–964. <https://doi.org/10.1016/j.watres.2003.11.009>
- Duan Y, Deng L, Shi Z, et al (2019) Assembly of graphene on Ag₃PO₄/AgI for effective degradation of carbamazepine under Visible-light irradiation: Mechanism and degradation pathways. *Chemical Engineering Journal* 359:1379–1390. <https://doi.org/10.1016/j.cej.2018.11.040>
- El Mouchtari EM, Daou C, Rafqah S, et al (2020) TiO₂ and activated carbon of Argania Spinosa tree nutshells composites for the adsorption photocatalysis removal of pharmaceuticals from aqueous solution. *Journal of Photochemistry and Photobiology A: Chemistry* 388:112183. <https://doi.org/10.1016/j.jphotochem.2019.112183>
- Fabbri D, López-Muñoz MJ, Daniele A, et al (2019) Photocatalytic abatement of emerging pollutants in pure water and wastewater effluent by TiO₂ and Ce-ZnO: degradation kinetics and assessment of transformation products. *Photochemical & Photobiological Sciences* 18:845–852. <https://doi.org/10.1039/C8PP00311D>
- Friedmann D, Mendive C, Bahnemann D (2010) TiO₂ for water treatment: Parameters affecting the kinetics and mechanisms of photocatalysis. *Applied Catalysis B: Environmental* 99:398–406. <https://doi.org/10.1016/j.apcatb.2010.05.014>
- Gerischer H, Heller A (1991) The role of oxygen in photooxidation of organic molecules on semiconductor particles. *The Journal of Physical Chemistry* 95:5261–5267. <https://doi.org/10.1021/j100166a063>

- Gode F, Atalay ED, Pehlivan E (2008) Removal of Cr(VI) from aqueous solutions using modified red pine sawdust. *Journal of Hazardous Materials* 152:1201–1207. <https://doi.org/10.1016/j.jhazmat.2007.07.104>
- Golan-Rozen N, Seiwert B, Riemenschneider C, et al (2015) Transformation Pathways of the Recalcitrant Pharmaceutical Compound Carbamazepine by the White-Rot Fungus *Pleurotus ostreatus* : Effects of Growth Conditions. *Environmental Science & Technology* 49:12351–12362. <https://doi.org/10.1021/acs.est.5b02222>
- Grzechulska J, Morawski AW (2002) Photocatalytic decomposition of azo-dye acid black 1 in water over modified titanium dioxide. *Applied Catalysis B: Environmental* 36:45–51. [https://doi.org/10.1016/S0926-3373\(01\)00275-2](https://doi.org/10.1016/S0926-3373(01)00275-2)
- Hübner U, Seiwert B, Reemtsma T, Jekel M (2014) Ozonation products of carbamazepine and their removal from secondary effluents by soil aquifer treatment – Indications from column experiments. *Water Research* 49:34–43. <https://doi.org/10.1016/j.watres.2013.11.016>
- Jelic A, Cruz-Morató C, Marco-Urrea E, et al (2012) Degradation of carbamazepine by *Trametes versicolor* in an air pulsed fluidized bed bioreactor and identification of intermediates. *Water Research* 46:955–964. <https://doi.org/10.1016/j.watres.2011.11.063>
- Jelic A, Michael I, Achilleos A, et al (2013) Transformation products and reaction pathways of carbamazepine during photocatalytic and sonophotocatalytic treatment. *Journal of Hazardous Materials* 263:177–186. <https://doi.org/10.1016/j.jhazmat.2013.07.068>
- Kosjek T, Andersen HR, Kompere B, et al (2009) Fate of Carbamazepine during Water Treatment. *Environmental Science & Technology* 43:6256–6261. <https://doi.org/10.1021/es900070h>
- Leary R, Westwood A (2011) Carbonaceous nanomaterials for the enhancement of TiO₂ photocatalysis. *Carbon* 49:741–772. <https://doi.org/10.1016/j.carbon.2010.10.010>
- Li Puma G, Bono A, Krishnaiah D, Collin JG (2008) Preparation of titanium dioxide photocatalyst loaded onto activated carbon support using chemical vapor deposition: A review paper. *Journal of Hazardous Materials* 157:209–219. <https://doi.org/10.1016/j.jhazmat.2008.01.040>
- Liu N, Lei Z-D, Wang T, et al (2016) Radiolysis of carbamazepine aqueous solution using electron beam irradiation combining with hydrogen peroxide: Efficiency and mechanism. *Chemical Engineering Journal* 295:484–493. <https://doi.org/10.1016/j.cej.2016.03.040>
- Maira AJ, Yeung KL, Soria J, et al (2001) Gas-phase photo-oxidation of toluene using nanometer-size TiO₂ catalysts. *Applied Catalysis B: Environmental* 29:327–336. [https://doi.org/10.1016/S0926-3373\(00\)00211-3](https://doi.org/10.1016/S0926-3373(00)00211-3)
- Matos J, Laine J, Herrmann J-M (2001) Effect of the Type of Activated Carbons on the Photocatalytic Degradation of Aqueous Organic Pollutants by UV-Irradiated Titania. *Journal of Catalysis* 200:10–20. <https://doi.org/10.1006/jcat.2001.3191>
- Matos J, Laine J, Herrmann J-M (1998) Synergy effect in the photocatalytic degradation of phenol on a suspended mixture of titania and activated carbon. *Applied Catalysis B: Environmental* 18:281–291. [https://doi.org/10.1016/S0926-3373\(98\)00051-4](https://doi.org/10.1016/S0926-3373(98)00051-4)
- Miao X-S, Metcalfe CD (2003) Determination of Carbamazepine and Its Metabolites in Aqueous Samples Using Liquid Chromatography–Electrospray Tandem Mass Spectrometry. *Analytical Chemistry* 75:3731–3738. <https://doi.org/10.1021/ac030082k>

- Moosavifar M, Bagheri S (2019) Photocatalytic Performance of $H_6 P_2 W_{18} O_{62} /TiO_2$ Nanocomposite Encapsulated into Beta Zeolite under UV Irradiation in the Degradation of Methyl Orange. *Photochemistry and Photobiology* 95:532–542. <https://doi.org/10.1111/php.13015>
- Nawaz M, Miran W, Jang J, Lee DS (2017) One-step hydrothermal synthesis of porous 3D reduced graphene oxide/TiO₂ aerogel for carbamazepine photodegradation in aqueous solution. *Applied Catalysis B: Environmental* 203:85–95. <https://doi.org/10.1016/j.apcatb.2016.10.007>
- Nigam M, Rajoriya S, Rani Singh S, Kumar P (2019) Adsorption of Cr (VI) ion from tannery wastewater on tea waste: Kinetics, equilibrium and thermodynamics studies. *Journal of Environmental Chemical Engineering* 7:103188. <https://doi.org/10.1016/j.jece.2019.103188>
- Ouyang J, Zhou L, Liu Z, et al (2020) Biomass-derived activated carbons for the removal of pharmaceutical micropollutants from wastewater: A review. *Separation and Purification Technology* 253:117536. <https://doi.org/10.1016/j.seppur.2020.117536>
- Pan Y, Cheng S, Yang X, et al (2017) UV/chlorine treatment of carbamazepine: Transformation products and their formation kinetics. *Water Research* 116:254–265. <https://doi.org/10.1016/j.watres.2017.03.033>
- Petrovic M, Petrovic M, Barceló D (2007) LC-MS for identifying photodegradation products of pharmaceuticals in the environment. *TrAC Trends in Analytical Chemistry* 26:486–493. <https://doi.org/10.1016/j.trac.2007.02.010>
- Qin Q, Chen X, Zhuang J (2015) The Fate and Impact of Pharmaceuticals and Personal Care Products in Agricultural Soils Irrigated With Reclaimed Water. *Critical Reviews in Environmental Science and Technology* 45:1379–1408. <https://doi.org/10.1080/10643389.2014.955628>
- Rodríguez-reinoso F (1998) The role of carbon materials in heterogeneous catalysis. *Carbon* 36:159–175. [https://doi.org/10.1016/S0008-6223\(97\)00173-5](https://doi.org/10.1016/S0008-6223(97)00173-5)
- Sopyan I, Watanabe M, Murasawa S, et al (1996) An efficient TiO₂ thin-film photocatalyst: photocatalytic properties in gas-phase acetaldehyde degradation. *Journal of Photochemistry and Photobiology A: Chemistry* 98:79–86. [https://doi.org/10.1016/1010-6030\(96\)04328-6](https://doi.org/10.1016/1010-6030(96)04328-6)
- Sunil R, Ahlaam H, Bhawna C, et al (2020) Influence of Adsorption Process Parameters on the Removal of Hexavalent Chromium (Cr(VI)) from Wastewater: A Review
- Tang L, Ma XY, Wang Y, et al (2020) Removal of trace organic pollutants (pharmaceuticals and pesticides) and reduction of biological effects from secondary effluent by typical granular activated carbon. *Science of The Total Environment* 749:141611. <https://doi.org/10.1016/j.scitotenv.2020.141611>
- Tang L, Wang J, Jia C, et al (2017) Simulated solar driven catalytic degradation of psychiatric drug carbamazepine with binary BiVO₄ heterostructures sensitized by graphene quantum dots. *Applied Catalysis B: Environmental* 205:587–596. <https://doi.org/10.1016/j.apcatb.2016.10.067>
- Tomasi J, Persico M (1994) Molecular Interactions in Solution: An Overview of Methods Based on Continuous Distributions of the Solvent. *Chemical Reviews* 94:2027–2094. <https://doi.org/10.1021/cr00031a013>
- Tryba B, Morawski AW, Inagaki M (2003) Application of TiO₂-mounted activated carbon to the removal of phenol from water. *Applied Catalysis B: Environmental* 41:427–433. [https://doi.org/10.1016/S0926-3373\(02\)00173-X](https://doi.org/10.1016/S0926-3373(02)00173-X)

- Uzunova M, Kostadinov M, Georgieva J, et al (2007) Photoelectrochemical characterisation and photocatalytic activity of composite La₂O₃-TiO₂ coatings on stainless steel. *Applied Catalysis B: Environmental* 73:23–33. <https://doi.org/10.1016/j.apcatb.2006.12.004>
- Valova E, Georgieva J, Armyanov S, et al (2010) Morphology, Structure and Photoelectrocatalytic Activity of TiO₂/WO₃ Coatings Obtained by Pulsed Electrodeposition onto Stainless Steel. *Journal of The Electrochemical Society* 157:D309. <https://doi.org/10.1149/1.3356001>
- Wei W, Yu C, Zhao Q, et al (2014) Synergy effect in photodegradation of contaminants from water using ordered mesoporous carbon-based titania catalyst. *Applied Catalysis B: Environmental* 146:151–161. <https://doi.org/10.1016/j.apcatb.2013.04.048>
- Xu J, Li L, Guo C, et al (2013) Photocatalytic degradation of carbamazepine by tailored BiPO₄: efficiency, intermediates and pathway. *Applied Catalysis B: Environmental* 130–131:285–292. <https://doi.org/10.1016/j.apcatb.2012.11.013>
- Yan SC, Li ZS, Zou ZG (2010) Photodegradation of Rhodamine B and Methyl Orange over Boron-Doped g-C₃N₄ under Visible Light Irradiation. *Langmuir* 26:3894–3901. <https://doi.org/10.1021/la904023j>
- Yang Y, Ok YS, Kim K-H, et al (2017) Occurrences and removal of pharmaceuticals and personal care products (PPCPs) in drinking water and water/sewage treatment plants: A review. *Science of The Total Environment* 596–597:303–320. <https://doi.org/10.1016/j.scitotenv.2017.04.102>
- Yao S, Jia Y, Shi Z, Zhao S (2010) Photocatalytic Oxidation of Arsenite by a Composite of Titanium Dioxide and Activated Carbon Fiber. *Photochemistry and Photobiology* 86:1215–1221. <https://doi.org/10.1111/j.1751-1097.2010.00813.x>
- Yoon S-H, Lee JH (2005) Oxidation Mechanism of As(III) in the UV/TiO₂ System: Evidence for a Direct Hole Oxidation Mechanism. *Environmental Science & Technology* 39:9695–9701. <https://doi.org/10.1021/es051148r>
- Zhai J, Wang Q, Li Q, et al (2018) Degradation mechanisms of carbamazepine by δ-MnO₂: Role of protonation of degradation intermediates. *Science of The Total Environment* 640–641:981–988. <https://doi.org/10.1016/j.scitotenv.2018.05.368>
- Zhang Y, Geißen S-U, Gal C (2008) Carbamazepine and diclofenac: Removal in wastewater treatment plants and occurrence in water bodies. *Chemosphere* 73:1151–1161. <https://doi.org/10.1016/j.chemosphere.2008.07.086>
- Zhao C, Liao Z, Liu W, et al (2020) Carbon quantum dots modified tubular g-C₃N₄ with enhanced photocatalytic activity for carbamazepine elimination: Mechanisms, degradation pathway and DFT calculation. *Journal of Hazardous Materials* 381:120957. <https://doi.org/10.1016/j.jhazmat.2019.120957>
- Zhu Z, Cai H, Sun D-W (2018) Titanium dioxide (TiO₂) photocatalysis technology for nonthermal inactivation of microorganisms in foods. *Trends in Food Science & Technology* 75:23–35. <https://doi.org/10.1016/j.tifs.2018.02.018>

Supplementary data

Insights in the aqueous and adsorbed photocatalytic degradation of carbamazepine by a biosourced composite: kinetics, mechanisms and DFT calculations.

El Mouchtari EL mountassir^(1,3), Bahsis Lahoucine^(1,2), El Mersly Lekbira⁽¹⁾, Anane Hafid⁽¹⁾, Lebarillier Stephanie⁽³⁾, Piram Anne⁽³⁾, Briche Samir⁽⁴⁾, Wong-Wah-Chung Pascal⁽³⁾, Rafqah Salah^{*(1)}.

⁽¹⁾ Laboratoire de Chimie Analytique et Moléculaire, Faculté Polydisciplinaire de Safi, Université Cadi Ayyad, Safi, Morocco

⁽²⁾ [Laboratoire de Chimie de Coordination et d'Analytique](#), Département de Chimie, Faculté des Sciences d'El Jadida, Université Chouaïb Doukkali, El Jadida, Morocco

⁽³⁾ Aix Marseille Univ, CNRS, LCE, Marseille, France

⁽⁴⁾ Département stockage de l'énergie et revêtements multifonctionnels, MAScIR, Rabat, Morocco.

* Corresponding author: [Pr. Salah RAFQAH](#) (E-mail : s.rafqah@uca.ma)

Laboratoire de Chimie Analytique et Moléculaire (LCAM)

Département de Chimie, Faculté Polydisciplinaire de Safi Université Cadi Ayyad.

Sidi Bouzid, B.P. 4162, 46000 Safi Maroc

Tel : 00-212-524669357 ;Fax : 00-212-524669516.

Table S1. Recovery of CBZ by extraction with MeOH

	Initial CBZ concentration (mg.L ⁻¹)	Equilibrium CBZ concentration (mg.L ⁻¹)	Amount of CBZ adsorbed (mg.L ⁻¹)	CBZ concentration after extraction (mg.L ⁻¹)	Recovery (%)	Average Recovery (%)
1	50.123	25.249	24.874	23.61	94.92	94.69
2	49.778	24.150	25.626	24.012	93.7	
3	51.014	25.741	25.273	24.128	95.46	

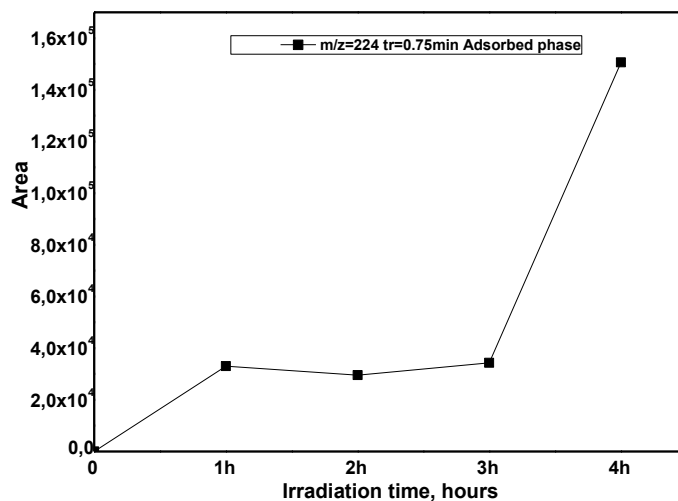
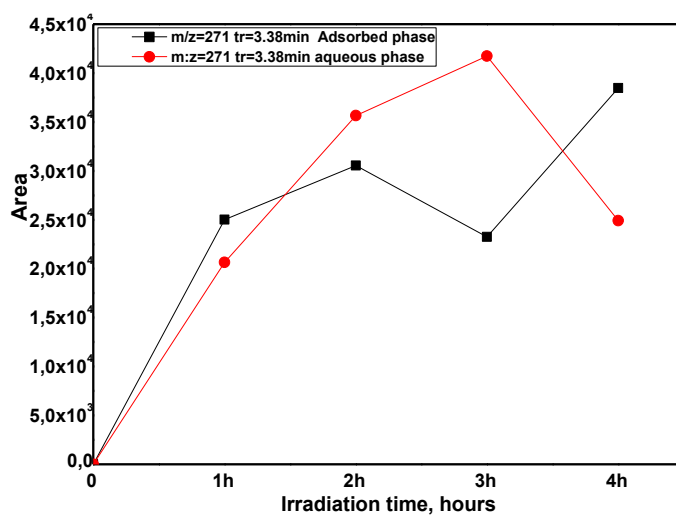
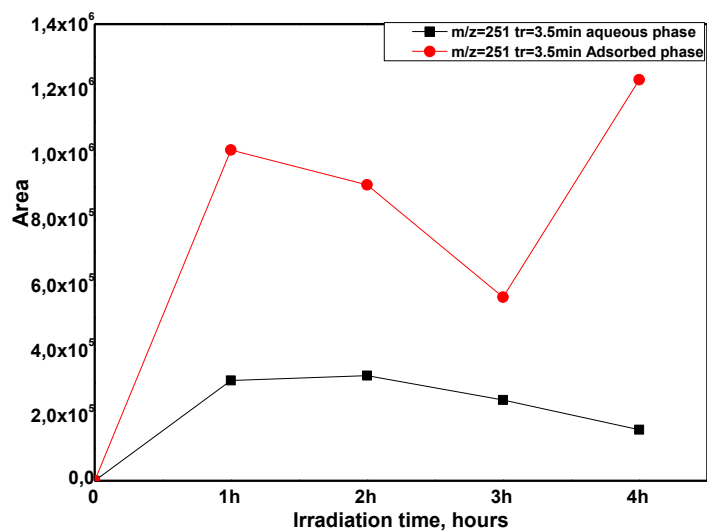


Fig S1. Kinetics of degradation of the TPs detected in aqueous solution and adsorbed on AC-TiO₂-9%

1. Theoretical background

Fukui function

Parr et *al.* proposed within the DFT method a new function named Fukui function for reactivity description of a molecule in which sites with the largest values of $f(r)$ are those with higher reactivity (1,2). The Fukui function was defined as:

$$f_k = \left[\frac{\partial \rho(r)}{\partial N} \right]_{v(r)}$$

Where N is the number of electrons and $\rho(r)$ is the electronic density.

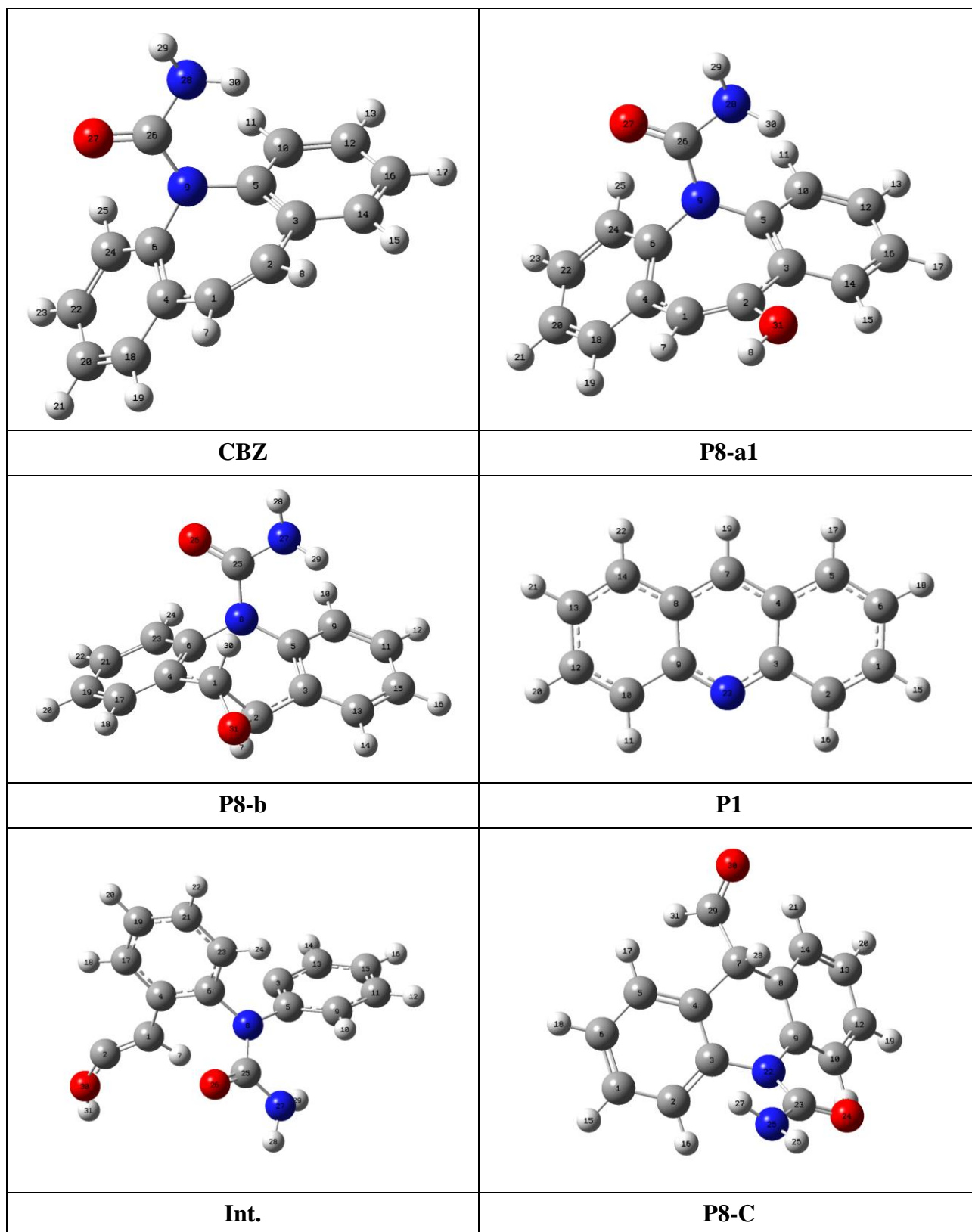
Although, in principle, the electron density of a neutral or $N_{0\pm\text{electron}}$ molecule contains all the information needed for the evaluation of the Fukui function $f(r)$, in which the Fukui functions $f(r)$ are approximated as: $f_k^- = [q_k(N) - q_k(N - 1)]$ for *electrophilic attacks* and $f_k^+ = [q_k(N+1) - q_k(N)]$ for *nucleophilic attacks* and $f_k^0 = 1/2(f_k^+ + f_k^-)$ for *radical attacks*. Where $q(N)$, $q(N + 1)$ and $q(N - 1)$ are the electron density on atom K on the neutral, anionic, and cationic species, respectively.

Morell et al. have proposed a local reactivity descriptor (LRD) which is called the dual descriptor $\Delta f(r)$ (3). The dual descriptor can be condensed over the atomic sites: when $\Delta f_k > 0$ the process is driven by a nucleophilic attack on atom k and then that atom acts as an electrophilic species. Conversely, when $\Delta f_k < 0$ the process is driven by an electrophilic attack over atom k and therefore atom k acts as a nucleophilic species. Thus, the Dual Descriptor was defined as:

$$\Delta f_k(r) = f_k^+ - f_k^-$$

In our study, Multiwfn was used to calculate dual descriptors for CBZ and selected intermediates (4).

2. Optimized structures of CBZ and selected intermediates



3. Fukui functions for P8-C and P1

Table S2. Fukui index distribution on P8-C calculated at B3LYP/6-31G(d,p) level.

Atom	No	f_k^+	f_k^-	f^o
C	1	0.02305	0.0151	0.019075
C	2	0.05012	0.03231	0.041215
C	3	0.10074	-0.00657	0.047085
C	4	0.00127	0.02532	0.013295
C	5	0.02033	0.01296	0.016645
C	6	0.10309	0.07798	0.090535
C	7	-0.0102	-0.00995	-0.010075
C	8	-0.01301	0.04127	0.01413
C	9	0.00134	0.02467	0.013005
C	10	0.01326	0.04039	0.026825
H	11	0.01799	0.02229	0.02014
C	12	0.03505	0.01563	0.02534
C	13	0.0272	0.10416	0.06568
C	14	-0.00306	0.01353	0.005235
H	15	0.0354	0.03019	0.032795
H	16	0.03223	0.01967	0.02595
H	17	0.01035	0.02438	0.017365
H	18	0.03681	0.02858	0.032695
H	19	0.02617	0.03351	0.02984
H	20	0.02411	0.03111	0.02761
H	21	-0.00181	0.02847	0.01333
N	22	-0.01026	0.17397	0.081855
C	23	0.00979	-0.02022	-0.005215
O	24	0.04287	0.08069	0.06178
N	25	0.00629	0.03882	0.022555
H	26	0.02252	0.02742	0.02497
H	27	-0.00332	0.01184	0.00426
H	28	0.02237	0.02824	0.025305
C	29	0.19666	-0.0193	0.08868
O	30	0.13793	0.05446	0.096195
H	31	0.04472	0.0191	0.03191

Table S3. Fukui index distribution on P1 intermediate calculated at B3LYP/6-31G(d,p) level.

Atom	No	f_k^+	f_k^-	f^o
C	1	0.05273	0.04691	0.04982
C	2	0.06179	0.08882	0.075305
C	3	0.00638	-0.01577	-0.004695
C	4	-0.0087	-0.01181	-0.010255
C	5	0.06223	0.0837	0.072965
C	6	0.04878	0.05769	0.053235
C	7	0.13314	0.10251	0.117825
C	8	-0.0087	-0.01181	-0.010255
C	9	0.00638	-0.01577	-0.004695
C	10	0.06179	0.08882	0.075305
H	11	0.03184	0.02869	0.030265
C	12	0.05273	0.04691	0.04982
C	13	0.04878	0.05769	0.053235
C	14	0.06223	0.0837	0.072965
H	15	0.03707	0.03477	0.03592
H	16	0.03184	0.02869	0.030265
H	17	0.03148	0.02945	0.030465
H	18	0.03691	0.03474	0.035825
H	19	0.03635	0.0283	0.032325
H	20	0.03707	0.03477	0.03592
H	21	0.03691	0.03474	0.035825
H	22	0.03148	0.02945	0.030465
N	23	0.1095	0.11477	0.112135

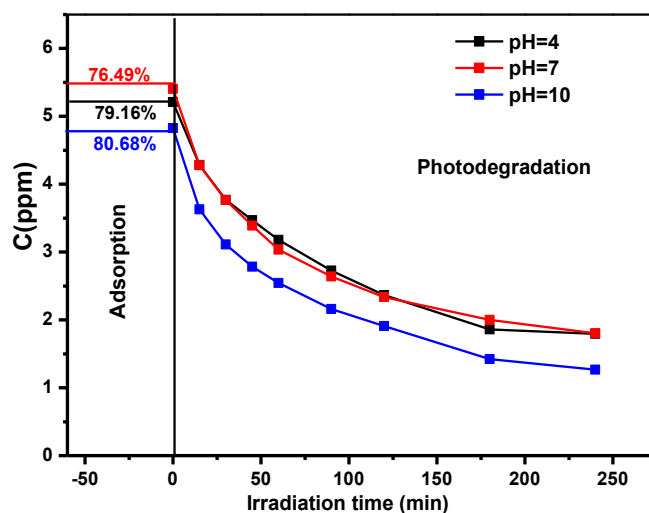


Figure S2. the effect of pH on adsorption and photocatalysis of CBZ in AC/TiO₂ 9%

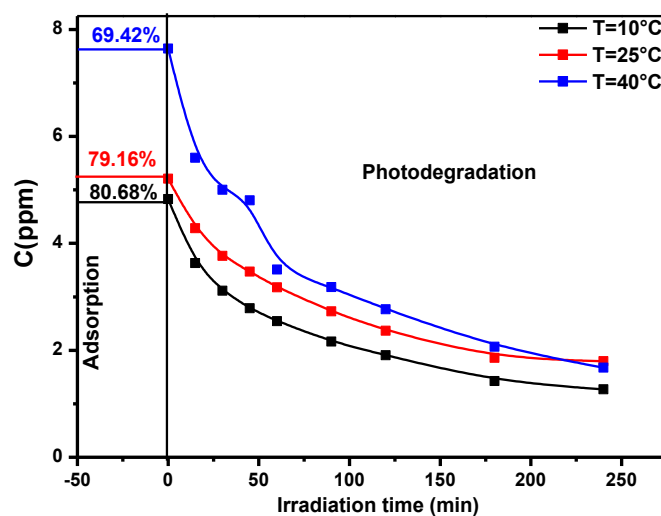


Figure S3. the effect of Temperature on adsorption and photocatalysis of CBZ in AC/TiO₂ 9%

References

1. Ayers, P. W. and Parr, R. G. (2000) Variational Principles for Describing Chemical Reactions: The Fukui Function and Chemical Hardness Revisited. *Journal of the American Chemical Society* **122**, 2010–2018. <https://doi.org/10.1021/ja9924039>.
2. Parr, R. G. and Yang, W. "*Density-functional theory of atoms and molecules*", Oxford University Press, **1989**.
3. Morell, C., Grand, A. and Toro-Labbé, A. (2006) Theoretical support for using the $\Delta f(r)$ descriptor. *Chemical Physics Letters* **425**, 342–346. <https://doi.org/10.1016/j.cplett.2006.05.003>.
4. Lu, T. and Chen, F. (2012) Multiwfn: A multifunctional wavefunction analyzer. *Journal of Computational Chemistry* **33**, 580–592. <https://doi.org/10.1002/jcc.22885>.